The elasmoid scales of teleosts: from structure to bioinspired materials

by

Louise ZYLBERBERG (1)

© SFI
Received: 7 Nov. 2017
Accepted: 13 Feb. 2018
Editor: O. Otero

Key words
Elasmoid scales
Structure
Mineralization
Teleosts
Bioinspired materials

Abstract. – The elasmoid scales of teleosts, remarkable by the diversity of their aspect and ornamentation, nevertheless present a similar structural organization. Each scale is composed of three superimposed layers. At the outer surface, the limiting layer, which may be absent in the anterior field, is the most mineralized of the three layers; it consists of a random meshwork of acidic glycoproteins. Collagen fibrils are the main component of the other two layers. The external layer is made up of thin collagen fibrils (30 nm in diameter) organized into a loose meshwork. This layer is the first to be formed and to be mineralized. Apatitic crystals are not coaligned with the thin collagen fibrils. The most extended part of the scale is the basal plate made up of thick collagen fibrils (about 100 nm in diameter), which are organized into a plywood-like structure. Apatitic crystals appear to be oriented in parallel to the direction of elongation of the fibrils, but they do not penetrate deeply within the fibrils. Most of the crystals are located in the interfibrillary matrix. Knowledge of the elasmoid scale structure may enable pathways to design bioinspired materials for various applications. Elasmoid scales are considered as a source of inspiration for biomimetic composites that would provide resistance, flexibility and lightweight. Because of their transparency and their composition in type I collagen, elasmoid scales are considered as a biomaterial useful for the repair of bone and cornea.

Résumé. – Les écailles élasmoïdes des téléostéens : leur structure, un modèle pour des matériaux bioinspirés.

Les écailles élasmoïdes des téléostéens dont la diversité de formes et d'ornementations superficielles sont remarquables, présentent néanmoins une structure similaire. Chaque écaille est composée de trois couches superposées. La couche la plus superficielle est la couche limitante qui peut être absente dans la partie antérieure de l'écaille. C'est la couche la plus minéralisée des trois couches, elle est formée d'un réseau de fines fibrilles où ont été identifiées des glycoprotéines acides. Les fibrilles de collagène sont le constituant essentiel des deux autres couches. La couche externe est une couche continue formée d'un enchevêtrement de fines fibrilles de collagène (diamètre 30 nm). Cette couche est la première formée, elle est aussi la première à être minéralisée. Les cristaux d'apatite ne sont pas alignés le long des fibrilles de collagène. La plaque basale représente la partie la plus importante d'une écaille élasmoïde. Elle est constituée de fibrilles de collagène de plus fort calibre (100 nm) que dans la couche externe. Les fibrilles de collagène sont disposées en strates superposées où elles sont parallèles les unes aux autres et leur orientation varie d'une strate à la suivante. Elles forment un contreplaqué biologique. Les cristaux d'apatite ont leur grand axe parallèle à celui des fibrilles de collagène auxquelles ils sont accolés. Ils forment un manchon autour des fibrilles et ne pénètrent que très peu à l'intérieur des fibrilles. La plupart des cristaux sont dans la matrice extrafibrillaire. Les acquis concernant la structure des écailles élasmoïdes sont à l'origine de recherches menant à la création de matériaux bioinspirés aux applications variées. Les écailles élasmoïdes sont considérées comme une source d'inspiration pour élaborer des composés biomimétiques qui auraient à la fois résistance, flexibilité et légèreté qui sont l'apanage des écailles élasmoïdes. Grâce à leur richesse en collagène de type I dont l'organisation leur confère une transparence les écailles se sont révélées comme un biomatériau pouvant être utile pour réparer le tissu osseux et la cornée.

In the 16th century, studies on actinopterygians and on their scales were stimulated by publications such as those of Belon du Mans (1551, 1555) and Rondelet (1558). From that time on, studies devoted to the scales have improved our knowledge of their structure. The use of scale morphology for actinopterygian classification can be traced back to the time of Agassiz (1833-1844). Studies increased in number and thoroughness during the late 19th century and the first half of the 20th century, with the advance of light microscopy (*e.g.* Mandl, 1839; Williamson, 1851; Baudelot, 1873; Goodrich, 1907; Cockerell, 1911; Lagler, 1947; Neave, 1936; Kobayashi, 1952-1953, 1953-1954, 1955; Wallin, 1956; Van Oosten, 1957). Later, the development of scanning electron microscopy (SEM) renewed our knowledge on the surface of the scales (*e.g.* DeLamater and Courtenay, 1974; Lanzing and Higginbotham, 1974; Hughes, 1981; Zylberberg and Meunier, 1981; Meunier, 1984; Lippitsch, 1990; Roberts, 1993; Voronina and Hughes, 2013). Since the middle of the 20th century, the development of transmission electron microscopy (TEM) triggered new studies on the ultrastructure of scales (*e.g.* Brown and Wellings, 1969; Maekawa and Yamada, 1970, 1972; Waterman, 1970; Yamada, 1971; Lan-

---

(1) Institut des Sciences de la Terre de Paris, CNRS UMR 7143 Sorbonne-Université, Université Pierre et Marie Curie, 4 place Jussieu, BC 19, 75005 Paris, France. [louise.zylberberg@upmc.fr]

zing and Higginbotham, 1976; Yamada and Watabe, 1979; Schönbörner *et al*., 1979, 1981; Frietsche and Bailey, 1980; Zylberberg and Nicolas, 1982; Sire and Géraudie, 1983; Zylberberg *et al*., 1992; Zylberberg and Meunier, 1996; Khemiri *et al*., 2001; Yang *et al*., 2014) and on scale regeneration (*e.g*. Neave, 1940; Sire and Géraudie, 1984; Bereiter-Hahn and Zylberberg, 1991; Ikoma *et al*., 2003; Ohira *et al*., 2007).

Studies on teleost scales were motivated by the belief that they could be used for classification, identification, age determination (Ombredane and Baglinière, 1991), and more recently, to develop design principles for engineered protective systems (Ikoma *et al*., 2003; Browning *et al*., 2013). Most studies, for whatever purposes, concern the highly derived elasmoid scales sheathing the body of most teleosts, the larger group of Actinopterygians with about 32,000 species described, indeed it represents about half of the whole vertebrates (Froese and Pauly 2017).

The elasmoid scales of teleosts display interesting combinations of flexibility, strength, lightweight, and transparency. These properties are thought to result from their structure, even though they exhibit a great diversity in shape, ranging from roughly circular to long oval, in size ranging from large to microscopic, and in superficial ornamentation. During the last decades, research on biological system such as elasmoid scales has revealed that these biological systems are arranged in a hierarchical multi-layered structure to achieve properties of high strength and lightweight. The purpose of this work is to gather data concerning the morphology and the structure of the teleost elasmoid scales acquired with histological and ultrastructural techniques. Knowledge of these structures may provide pathways to design bioinspired composite materials and suggest various applications.

STRUCTURAL CHARACTERISTICS OF ELASMOID SCALES IN TELEOSTS

General organization of elasmoid scales

The scales examined belong to the elasmoid type as defined by Bertin (1944): elasmoid scales are thin, transparent, flexible and lamellar plates most often imbricated.

1
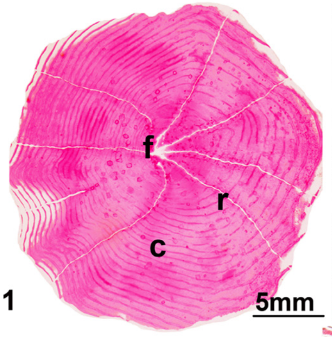

2
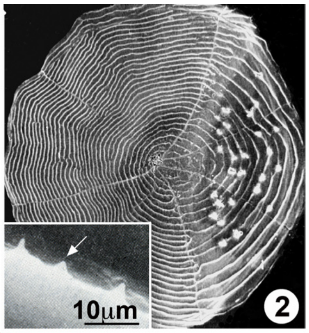

3
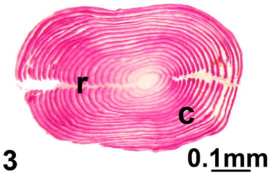

4
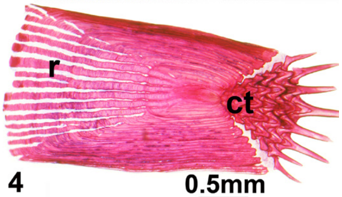

5
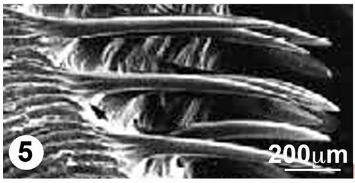

6
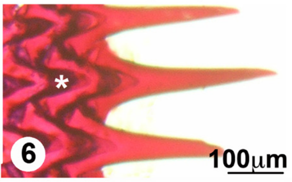

7
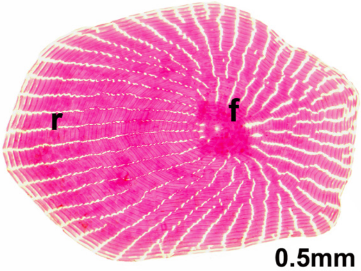

8
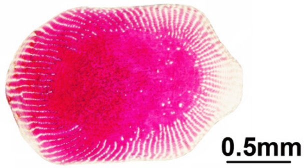

9
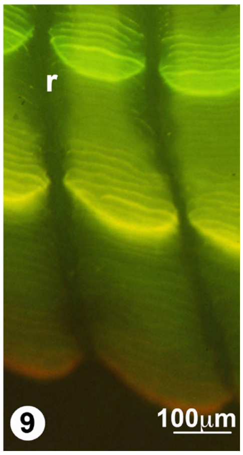

Figures 1-8. – Morphological aspects of elasmoid scales.
Figures 1, 2. – Cycloid Scale of *Carassius auratus*. **1**: Scale stained with alizarin red S. **2**: SEM. The circuli (c) are more spaced in the exposed posterior field than in the overlapped anterior field. Insert: Note the presence of denticles (arrow) on the apex of the circuli. c: circuli; f: focus of the scale; r: radius.
Figure 3. – Cycloid scale of *Gaidropsarus vulgaris* stained with alizarin red S. The circuli form regularly spaced out ridges concentrically disposed around the focus of the scale. The radii are oriented along the anteroposterior axis of the scale.
Figure 4. – Ctenoid scale of *Solea solea* stained with alizarin red S. The posterior part of the scale is ornamented with denticles: the cteni (ct). The radii (r) are parallel and oriented along the anteroposterior axis of the scale.
Figure 5. – SEM. Detail of the posterior part of the ctenoid scale of *Coryphaenoides rupestris,* which bears long fusiform cteni.
Figure 6. – Posterior part of a scale of *Solea solea* stained with alizarin red S. At the margin of the scale, the most recent ctenii form acute denticles whereas the oldest progressively resorbed appear as truncated spines (asterisk).
Figure 7. – Cycloid scale of *Trisopterus luscus* (Linnaeus, 1758) stained with alizarin red S. Numerous radii (r) span out from the focus (f) to the periphery of the scale.
Figure 8. – Regenerating scale of *Trisopterus luscus* stained with alizarin red S showing an organization resembling that of the regular developed scales (Fig. 7).
Figure 9. – Scale growth. Labelling in successive times with three different fluorochromes of a scale of *Hemichromis bimaculatus* Gill, 1862, fluoresceine: yellow-green, tetracycline: yellow and xylelol orange: red, reveals the successive mineral deposits during the scale growth. The unmineralized radii (r) are not labelled (micrograph: F.J. Meunier).

The association of *in toto* staining with alizarin red S (Francillon and Meunier, 1985), that shows the extend of mineralization, and scanning electron microscopy (SEM) have proved to be very effective in demonstrating the variety of the surface ornamentations of scales.

Because of their overlap, the elasmoid scales show two distinct regions, which develop different superficial ornamentations (Fig. 1A, B). The posterior field, the exposed area of the scale lying below the epidermis, differs from the anterior and lateral areas, which are covered by the adjacent scales. The anterior field is deeply inserted within the dermis. The boundary between the anterior (overlapped) and the posterior (exposed) fields observed in SEM is shown in figure 1B.

The surface ornamentation consists in the characteristic circuli, concentric crests separated by grooves surrounding the focus (Figs 1A, B, 2, 3, 6). The apex of the crest bears denticles oriented towards the focus (Fig. 1B insert). The circuli are interrupted by the unmineralized radii, which are the most flexible parts of the scales (Figs 1, 3, 4, 7). The radii arise from the focus and reach the scale margin. The radii may be distributed over all, or only part of the surface of the scale. In the small scales of *Gaidropsarus vulgaris* (Cloquet, 1924), the radii consist of two grooves parallel to the anterior-posterior axis of the scale (Fig. 2). In the oblong ctenoid scale of *Solea solea* (Linnaeus 1758), the parallel radii are oriented along an anteroposterior axis of the scale (Fig. 3). The ctenoid scales (Figs 4-6) differ from cycloid scales by the presence of comb-like structures on the posterior field (Figs 4-6).

The posterior margin of the ctenoid scales of *Solea solea* bears the cteni that are the most recently formed, whereas the oldest cteni are progressively resorbed, appear truncated. From the posterior margin towards the focus of the scale, the cteni (eroded or not) are arranged in longitudinal rows (Fig. 6).

Numerous comb-like ctenii cover the whole posterior field of the scales of the gadid *Coryphaenoides rupestris* Gunnerus, 1765. They are fusiform, about 1.5 mm in length, and with a sharp tip. The cteni, which are in the vicinity of the circuli, appear to be connected with them (Fig. 5).

The scales of teleosts regenerate when they are damaged or lost. The basic organization of the regenerating scale resembles that of the original ones (Figs 7, 8). However, the peculiar aspect of the focus of early regenerating scales is thought to be related to a decrease of the control of the scale pattern due to the faster development of regenerating scales.

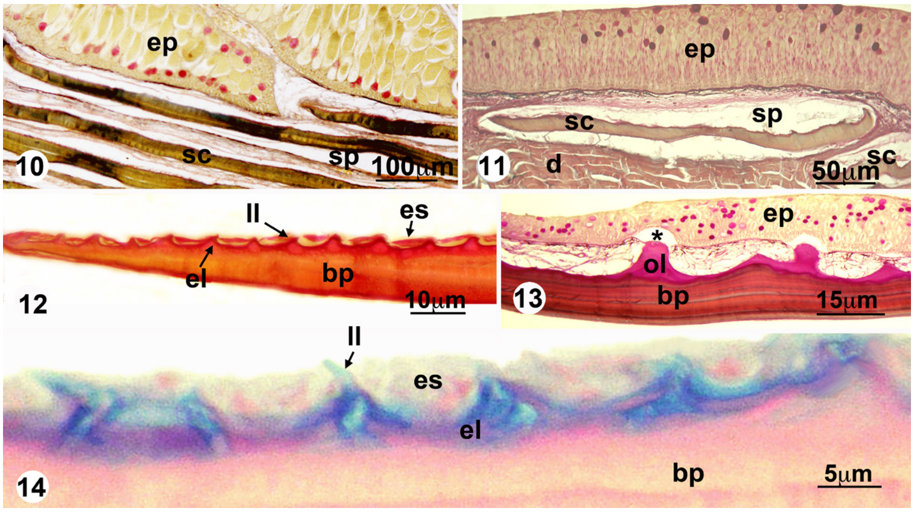

Figures 10-14 – The histological techniques were carried following Gabe (1968) and Lillie and Fulmer (1976) procedures.
Figure 10. – *Tinca tinca* (Linnaeus, 1758). PAS - Groat's hematoxylin - picroindigocarmine. Vertical section of the skin showing superimposed scales (sc), each scale is inserted in its pocket (sp). ep: epidermis.
Figure 11. - *Anguilla anguilla* (Linnaeus, 1758). PAS – Groat's hematoxylin – picroindigocarmine. Vertical section of the skin showing scales (sc) arranged side by side. Each scale is inserted in its pocket (sp). ep: epidermis; d: dermis.
Figure 12. – *Cyprinus carpio* Linnaeus, 1758. PAS – Groat's hematoxylin. Vertical section in the anterior field. Episquamal scleroblasts (es) are inserted between two circuli. bp: basal plate; el: external layer.
Figure 13. – *Cyprinus carpio*. PAS - Groat's hematoxylin – picroindigocarmine. Vertical section in the posterior field. PAS-positive elevations are formed by the osseous layer (ol). The space (asterisk) is an artefact occurring during the preparation of the sample. The lamellar structure of the basal plate (bp) is obvious. ep: epidermis
Figure 14. – *Cyprinus carpio*. Alcian blue – nuclear fast red. Vertical section in the posterior field showing circuli. The limiting layer (ll) and the external layer (el) are stained in blue. The basal plate (bp) does not contain material stained with Alcian blue.

In teleosts, the elasmoid scales grow and are mineralized through life, increasing both in surface areas at the periphery and in thickness.

The scale growth towards the periphery is illustrated by the use of various fluorochromes (Fig. 9) that bind to calcium (Frost and Villaneuva, 1960; Frost, 1969; Francillon and Meunier, 1985; Pautke *et al*., 2005; van Gaalen, 2010). They are sequentially administered to visualise the direction of the new mineral deposit (Meunier, 1972, 1974). Meunier and Boivin (1978) have shown that the fluorochromes deposited at the site of active mineralization give information regarding the speed and the direction of mineralization during scale growth.

In arrangement, most often, the imbricated scales lie obliquely within the dermis (Fig. 10). In some teleosts, the pattern is mosaic; the scales are minutely separated or meet their neighbours only at their margin (Fig. 11). Whatever their arrangement is, each scale is inserted into a scale pocket (Whitear, 1986), which is delimited by the scale pocket cells. Vertical cross sections (in this study, vertical sections refer to sections perpendicular to the scale surface) show that a typical elasmoid scale is composed of two superimposed layers, a superficial osseous layer topping a thick and lamellar basal plate organized into a plywood-like structure (Zylberberg *et al.*, 1991). The basal plate is composed of superimposed plies within which the collagen fibrils are parallel one to another, but their direction changes from one ply to the next (Giraud *et al.*, 1978; Meunier and Géraudie, 1980). This organization in a plywood pattern was described by Meunier and Castanet (1982) in the elasmoid scales of teleosts and it was called elasmodin by Schultze (1996, present issue), who does not hint an odontogenic origin for this lamellar layer (Sire *et al.*, 2009). According to Schultze (1996, present issue), the plywood structure of the elasmoid scale differs in formation from isopedin, which is also composed of collagen fibrils organized in a plywood-like structure. In isopedin, found in bone and in the bony base of ganoid scales, osteocytes are involved in the mineralization that occurs as the collagenous matrix is laid down, whereas elasmodin of the basal plate is deposited after the formation of the external layer. Thus, its initial deposition is not mineralized and remains at least in part unmineralized. Cells, when present, are not involved in the mineralization. Because of their structural similarities, isopedin and elasmodin are considered as homoplastic tissues by Sire and Huysseune (2003).

The lightly P.A.S. (periodic acid-Schiff reagent) positive elasmodin of the basal plate contains glycoproteins, whereas the superficial osseous layer contains glycoproteins, but also acid mucopolysaccharides stained with Alcian blue (Figs 12-14). The superficial ornamentation of the scales is related to the organization and the thickness of the osseous layer. The osseous layer is composed of two layers: the limiting layer (the outer limiting layer of Schönbörner *et al.*, 1979) and the external layer. The limiting layer topping the external layer is often limited to the posterior field of the scale. The external layer forms an uninterrupted cover over the whole scale surface.

The scale-forming cells coined scleroblasts by Klaatsch (1890) line the scale surface. Later, Waterman (1970) suggested a terminology based on the topographical relationships of these cells to the scale: the episquama is composed of the scleroblasts covering the superficial surface, the hyposquama is composed of the scleroblasts underlying the deep surface, and the peripheral cells form a rim around the margin of the scales (Figs 15, 16). The terminology established by Waterman (1970) will be used in this article.

The external layer

At the margin of the scales, the external layer is surrounded by the peripheral scleroblasts that synthesize the thin collagen fibrils organized into a thin meshwork in the first step of the formation of the external layer. The external layer is the first layer to be formed (Fig. 16).

Episquamal scleroblasts can be anchored to a groove between two circuli (Fig. 17A, B), but generally, the episquamal scleroblasts are separated from each other by the serrations of the scale surface. Their shape is outlined by immunofluoresce using anti-actin and anti-tubulin antibodies (Zylberberg *et al.*, 1988). In *Carassius auratus* (Linnaeus, 1758), the newly thin collagen fibrils of about 30 nm in diameter are synthesized by the episquamal scleroblasts (Fig. 18); they are coaligned with the cytoskeleton elements located in the peripheral cytoplasm of the scleroblast lining the external layer (Fig. 19).

The mineral deposit appears in the external layer at the margin of the scale and at the top of the elevations forming the circuli (Fig. 20). The initial mineral deposit appears in form of small needle-shaped rodlets (Fig. 21). The rodlets are about 100 nm long in specimens, fixed with rapid freeze-fixation (Zylberberg and Nicolas, 1982). The mineral rodlets are mostly located in the interfibrillary matrix; they do not seem to be oriented by the thin collagen fibrils (30 nm in diameter), but their formation might be initiated by dense granules (Fig. 22).

Mineralization then proceeds by aggregation of the rodlets that form clusters (Fig. 22). The size of the clusters increases by aggregation of rodlets, whereas the size of each crystallite does not increase (Fig. 22). Finally, the clusters fuse to form a fully mineralized layer (Fig. 23). Once mineralized, the external layer is topped by the limiting layer that forms last. The limiting layer is covered by flattened episquamal scleroblasts, that can be anchored in the cavity inside a circulus (Fig. 24). This layer is devoid of collagen fibrils, but it contains abundant acid mucopolysaccharides, which form a microfibrillar matrix orienting the deposit of the mineral crystals (Fig. 25). The presence of bands distinguished by their difference of opacity to electrons indicates that the limiting layer is cyclically deposited (Fig. 26).

Bundles of closely packed collagen fibrils oriented parallel to each other arise from the external layer and cross the limiting layer (Fig. 26). These fibre bundles showing structural similarities with the fibres of attachment described in bone by Sharpey were considered as Sharpey fibre-like bundles (Zylberberg and Meunier, 1981). Only the part of the collagen fibrils inserted in the scale is mineralized.

The basal plate

The basal plate is the most extended part of the scale; it consists of elasmodin composed of several superimposed plies parallel to the surface of the scale (Fig. 27). In each

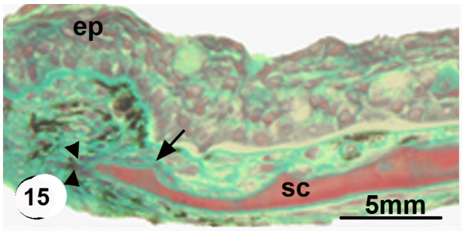

Figure 15. – *Cyprinus carpio*. One step trichrome. Vertical section of the anterior margin of the scale. A thick membrane stained in green is observed between the epidermis and the dermis. Within the dermis, the peripheral scleroblasts form a rim around the margin of the scale (arrowheads). The elevation corresponds to the formation of the first circulus (arrow).

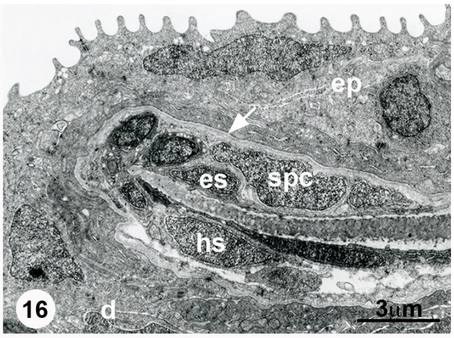

Figure 16. – *Carassius auratus*. TEM. Section of the margin of the scale. A thin microfibrillar membrane (arrow) separates the epidermis (ep) from the dermis (d). Scale pocket cells (spc) form a rim around the scales and line the scleroblasts. The external layer, the first layer to be formed, is deposited between the episquamal scleroblasts (es) and the hyposquamal scleroblasts (hs).

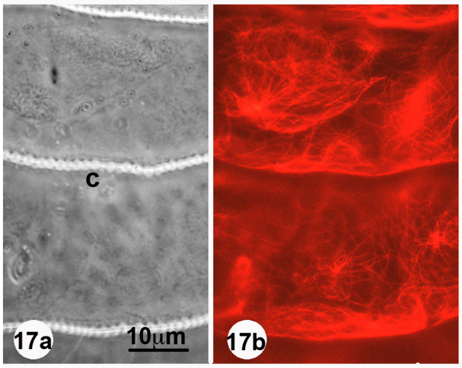

Figure 17. – *Carassius auratus*. Indirect immunofluorescence visualising microtubules in the episquamal scleroblasts. **A**: Phase constraste. **B**: Tyr-tubulin Mts distribution. Mts radiate from the MTOCs (microtubule organising centre) in cells located between two circuli (c).

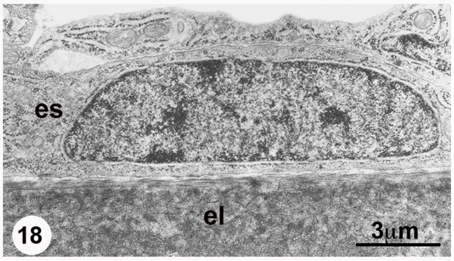

Figure 18. – *Carassius auratus*. TEM. Episquamal scleroblats lining the external layer.

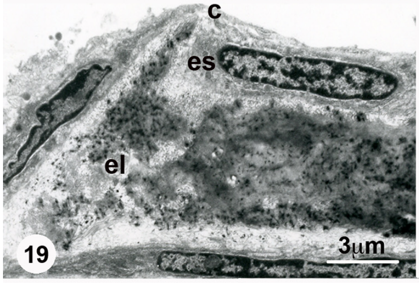

Figure 19. – Margin of the scale. Elevation of the external layer forming a circulus (c).

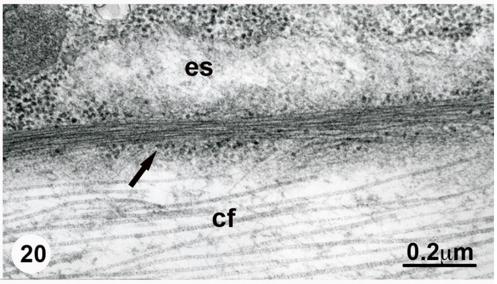

Figure 20. – *Carassius auratus*. TEM. Episquamal scleroblast (es) where cytoskeletal elements are coaligned with the thin collagen fibrils (cf).

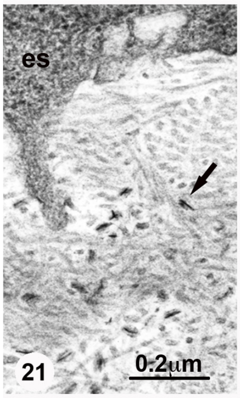

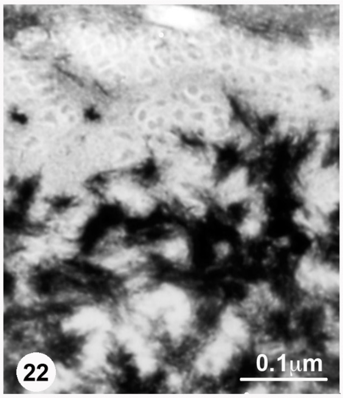

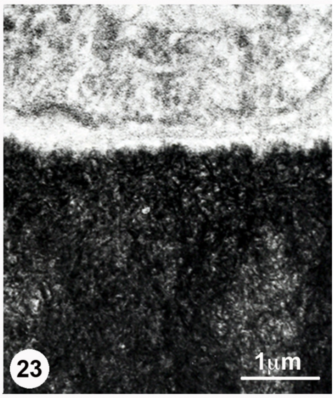

Figures 21-23. – *Carassius auratus*. TEM. Scales treated with rapid freeze-fixative procedures. Mineralization of the external layer. **21**: Needle-shaped crystals are deposited in the interfibrillary spaces (arrow). **22**: Clusters of crystals are randomly dispersed. **23**: Mineralized external layer.

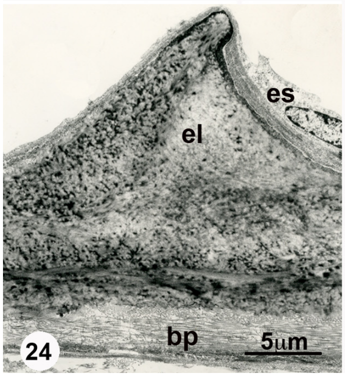

Figure 24. – *Carassius auratus*. TEM. Section of a partially demineralized circulus. The external layer (el) is composed of network of randomly dispersed collagen fibrils. A thin layer of microfibrillar material is deposited on one side of the circulus. bp: basal plate; es: episquamal scleroblast.

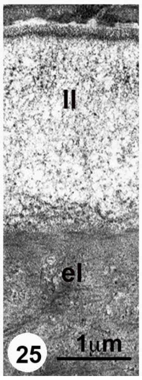

Figure 25. – *Carassius auratus*. TEM. Demineralized section. Detail of the organic material of the limiting layer (ll) made of a thin microfibrillar meshwork and the external layer (el) composed of thin collagen fibrils embedded in a matrix.

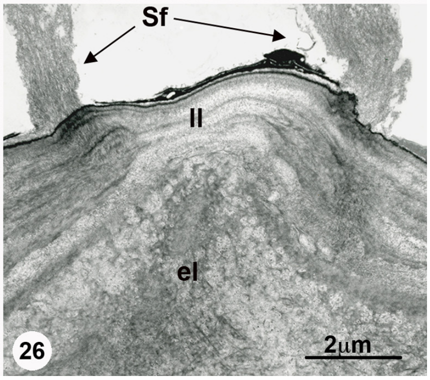

Figure 26. – *Cyprinus carpio*. TEM. Demineralized section of the upper part of the scale. Bundles of collagen fibres forming Sharpey-fibre-like bundles (Sf) cross the external layer (el) and the limiting layer (ll).

ply, the fibrils are parallel to one another but their direction changes from one ply to the next; this rotation is observed with polarised light (Fig. 27) and with SEM (Fig. 28). The direction of the fibrils is orthogonal from one ply to the next, thus forming an orthogonal plywood that shows two preferential directions (Fig. 29). The collagen fibrils are composed mainly of type I collagen associated with Type V collagen, which regulate the thickness of the fibrils (Zylberberg *et*

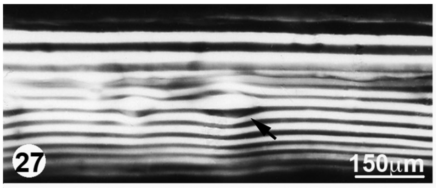

Figure 27. – *Etelis carbunculus* Cuvier, 1828. Ground section. Polarised light. Black and white superimposed collagenous plies are characteristic of an orthogonal plywood-like structure. The basal plate (bp) is partially mineralized. Mandl corpuscles (arrow) are observed at the level of the front of mineralization. (micrograph: F.J. Meunier).

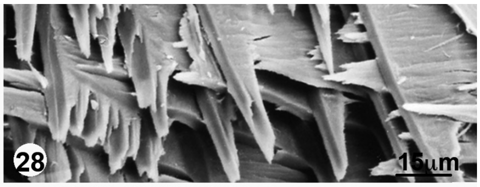

Figure 28. – *Macrourus berglax* Lacepède, 1801. SEM. Broken freezed scale showing the lamellar structure of the basal plate. The direction of the collagen fibrils of adjacent layers are at right angle to one another forming an orthogonal plywood-like structure.

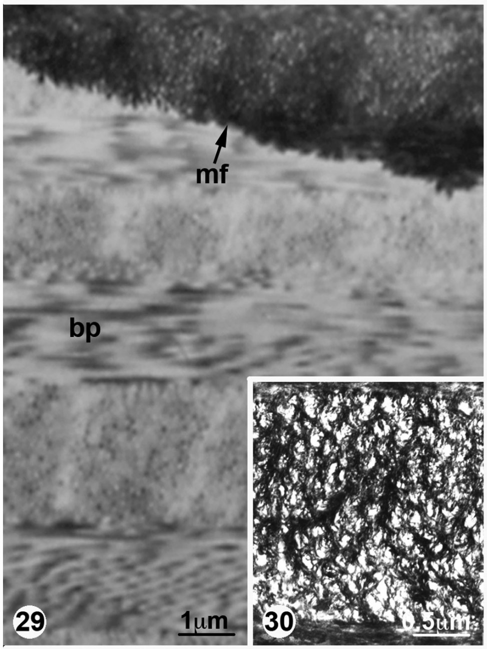

Figure 29. – *Poecilia reticulata* Peters, 1859. TEM. Rapid freeze anhydrous techniques. Front of mineralization (mf) in the basal plate (bp).

Figure 30. – *Poecilia reticulata*. TEM. Rapid freeze anhydrous techniques. The crystals are located in the spaces surrounding the cross-sectioned collagen fibrils that appear electrolucent.

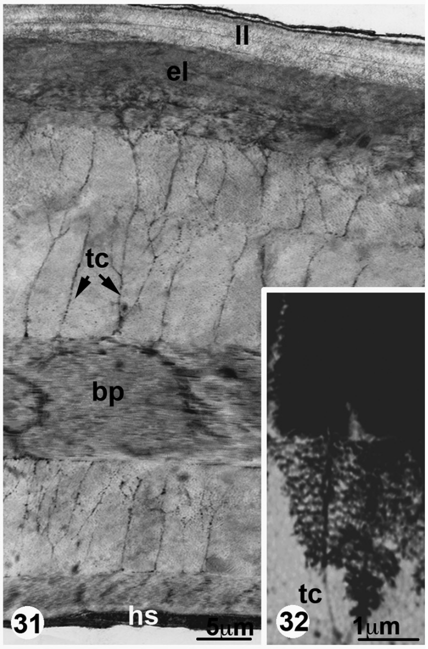

Figure 31. – *Carassius auratus*. TEM. Demineralized section. The superimposed plies of the basal plate (bp) are crossed by the TC fibres (tc) that arise from the hyposquamal scleroblasts (hs) and reach the external layer (el). ll: limiting layer

Figure 32. – *Carassius auratus*. TEM. Rapid freeze anhydrous techniques. The characteristic aspect of the front of mineralization is due to the presence of the TC fibres (tc). It differs from the smooth one of *Poecilia reticulata*, which has no TC fibers (Fig. 29).

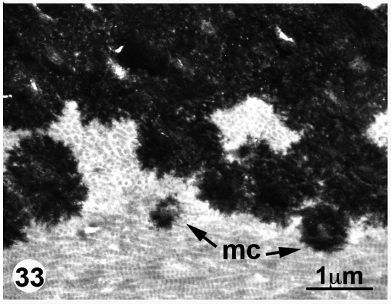

Figure 33. – *Poecilia reticulata*. TEM. Mineralized corpuscles, Mandl corpuscles (mc), are located ahead of the front of mineralization.

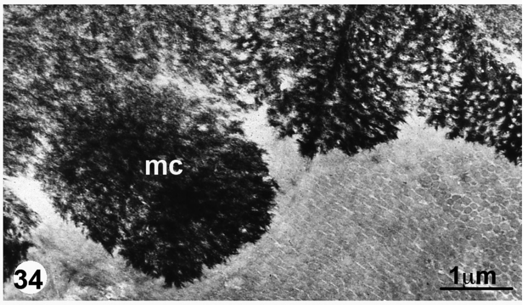

Figure 34. – *Carassius auratus*. TEM. Mandl corpuscles (mc) located ahead of the front of mineralization.

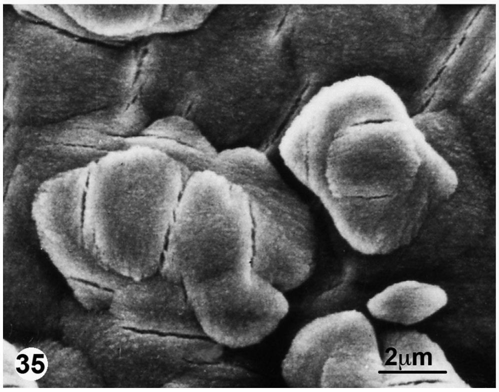

Figure 35. – *Trisopterus luscus*. SEM. The front of mineralization is ornamented with fused Mandl corpuscles.

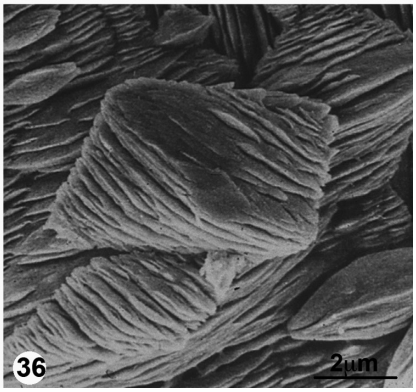

Figure 36. – *Cyprinus carpio*. SEM. Mandl corpuscles and the mineralization front show a ridged surface due to the presence of TC fibres.

al., 1992; Le Guellec and Zylberberg, 1998). The fibrils are about 100 nm in diameter. A more complex organization is observed in the basal plate, where the collagen fibrils form two imbricated systems of plies (the odd and the even, which constitute a double-twisted plywood-like structure (Meunier and Castanet, 1982; Meunier, 1984) (Fig. 31).

In the Cyprinidae, another network composed of thinner collagen fibrils, forms a "sheet-like structure", the "TC" fibres (Onozato and Watabe, 1979), that cross-fibrous plies of the basal plate (Figs 31, 32). Apart from their orientation, the TC fibres are also distinguishable from the other collagen fibrils of the basal plate by a definite difference in diameter; the TC fibres reach only 30 nm in diameter at the most (Fig. 31).

Anhydrous techniques for TEM show that the crystals of hydroxyapatite have their major axis oriented parallel to the elongation of the collagen fibrils. The mineral deposits enhance the periodicity of the collagen fibrils. Cross sections of the collagen fibrils reveal that the crystals invade the interfibrillar spaces and seem to be located around the collagen fibrils whose centres appear as electrolucent circular spaces (Figs 30, 32). The TC fibres are mineralized more rapidly than the fibrils of the plywood-like structure (Fig. 32). Indeed, the mineral deposit appears to be located initially along the TC fibres. The TC fibres mineralize before the thick collagen fibrils of the plywood-like structure. Therefore, the mineralization front resembles inverted trees (Fig. 32), whereas the mineralizing front appears as a smooth surface in basal plates devoid of TC fibres (Fig. 29).

The mineralization front is preceded by independently mineralized, approximately globular structures: Mandl corpuscles (Mandl, 1839). They form without any contact with a preexisting mineralized tissue (Figs. 33-36). They vary in size and shape, which are related to the organization of the plywood-like structure (Schönbörner *et al*., 1981). They show a ridged surface in scales with TC fibres (Fig. 36). The mineralization of Mandl corpuscles conforms to that of the plywood-like structure: the crystals are oriented by the collagen fibrils (Schönbörner *et al*., 1981; Zylberberg and Nicolas, 1982).

In fully developed scales where the rate of collagen deposition is slow and therefore the contribution of the scleroblast structure to fibril orientation is difficult to assess, studies were carried out on regenerating scales, which have a highly active fibrillogenesis.

The hyposquamal scleroblasts of developed scales are very thin (3 to 5 µm thick); they contain a central flattened nucleus (Fig. 37). The cytoskeletal elements underlying the secretory cell membrane are coaligned with the most recently synthesized collagen fibrils (Figs 38-40). In regenerating scales, the hyposquamal scleroblasts appeared as tall priamatic cells (15 µm high) and contain a globular nucleus of about 5 µm in diameter (Fig. 41). Gap junctions are frequent in freeze-fracture replicas (Fig. 42). Coincidence of the alignment of the cytoskeletal elements and that of the collagen fibrils in the ply in contact with the hyposquamal scleroblasts is obvious in TEM micrographs (Figs 43, 44).

To maintain the relationship between cytoskeletal elements and the collagen fibrils in the neighbour of the plasma membrane, the cyclic orientation changes of the collagen fibrils require a concomitant rearrangement of the cytoskeletal structure (Byers *et al*., 1980; Dane and Tucker, 1986; Zylberberg *et al*., 1988). In regenerating scales approximately one ply per day is deposited (Frietsche and Bailey, 1980), while synthesis is very slow in fully-grown scales. According to these observations a network of short-living microtubules (Mts) in regenerating scales and very stable ones in fully grown scales. Two specific antibodies have been used to differentiate such microtubules subsets.

In living cells, tubulin incorporated into Mts seems to be subjected continuously to chemical modifications: detyrosination by a carbopeptidase and retyronisation of monomeric a-tubulin by a ligase. Detyronisation is a slow process occurring in Mts while depolymerized tubulin only becomes (re-) tyrosinated. Therefore, Mts containing detyrosinated tubulin with glutamic acid at its carboxyl end (Glu-Mts) can be supposed to have existed for a longer time than those containing only a-tubulin with tyrosine at its carboxyl end (Tyr-Mts) (Gundersen *et al*., 1984). In the hyposquamal scleroblasts of well-developed scales, the Mts are labelled with both antibodies (Fig. 45A, B, C). In the hyposquamal scleroblasts of regenerating scales, which are known to have a high synthetic activity, only Tyr-Mts have been identified (Fig. 46A, B, C) (Zylberberg *et al*., 1991). The distribution of the two Mt populations is consistent with a turnover in the hyposquamal scleroblasts and support the hypothesis that a changing Mt pattern is involved in the generation of the collagen plywood.

ELASMOID SCALES AS A MODEL THAT COULD INSPIRE NOVEL ENGINEERING MATERIALS

Over the past few decades, there has been growing interest in natural materials whose structural characteristic are believed to underlie the good performance of various natural structures, to develop new synthetic materials. It is well known that the scaled integument of teleost displays interesting combinations of flexibility, strength, resistance to penetration, lightweight and transparency (Burdak, 1979; Currey, 1999). In addition to hydrodynamic properties crucial for swimming efficiency (Burdak, 1979; Sudo *et al*., 2002), elasmoid scales form a protective layer against predators or other mechanical threats. Studies on the structure and mechanics of elasmoid scales that involve tensile testing (Ikoma *et al*., 2003; Zhu *et al*., 2012; Garrano *et al*.,

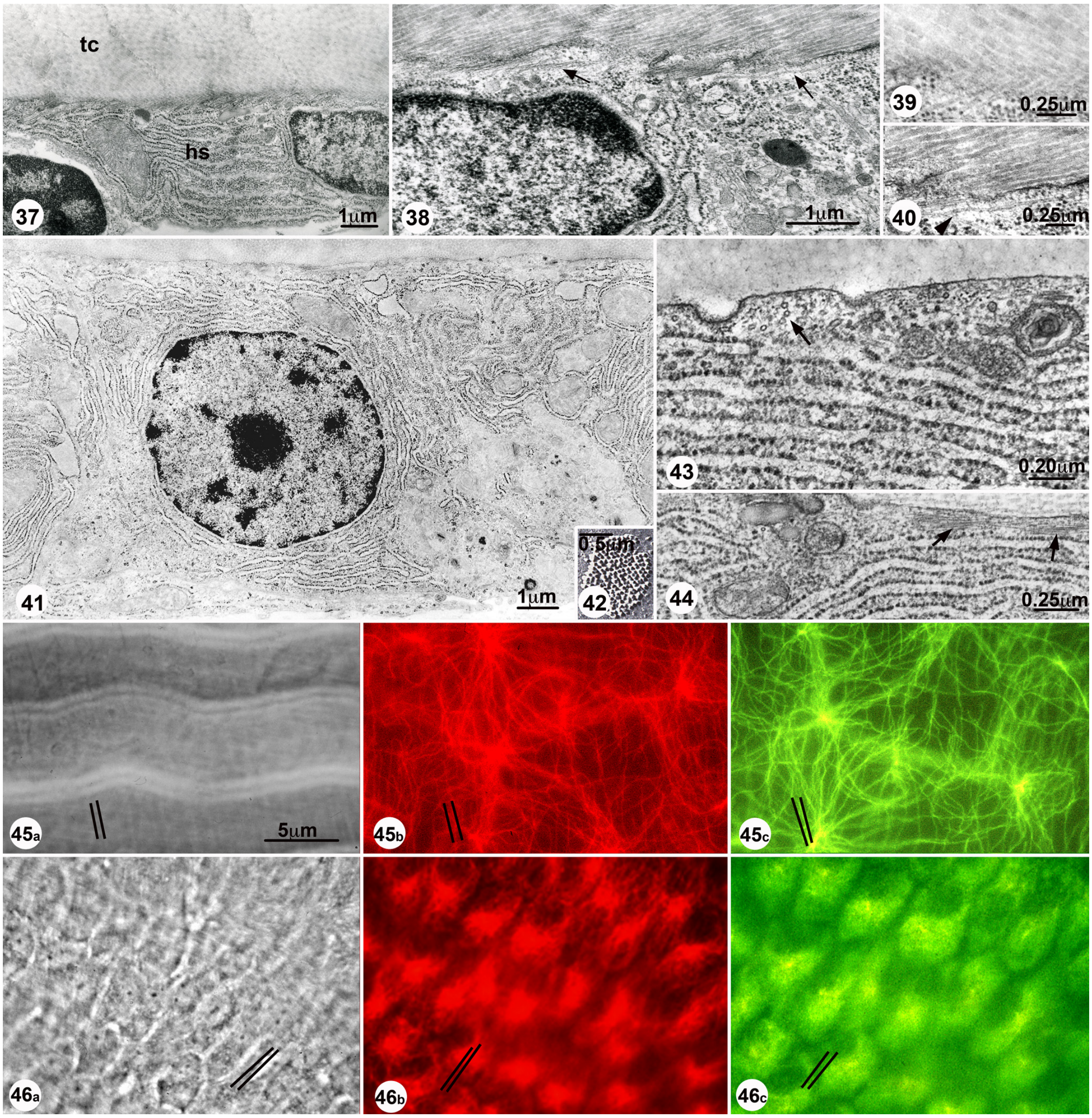

Figures 37-46. – *Carassius auratus*.
Figures 37-40. – TEM Control scales.
Figure 37. – Flat hyposquamal scleroblasts (hs) synthesise the thick collagen fibrils of the plywood-like structure of the basal plate and the thin TC fibres (tc) crossing the plywood-like structure.
Figure 38. – Collagen fibrils are coaligned with the Mts and microfilaments (arrows) underlying the plasma membrane of the hyposquamal scleroblast.
Figure 39. – Detail of the secretory surface of a hyposquamal scleroblast. The microfibrils and the Mts have changed their direction and are coaligned with the newly synthesized collagen fibrils forming a new layer.
Figure 40. – Detail of the secretory surface of a hyposquamal scleroblast. Mts (arrowhead) located in the vicinity of the plasma membrane are in parallel with the innermost thick collagen fibrils.
Figures 41- 44. – Four-day-regenerating scale.
Figure 41. – TEM. The hyposquamal scleroblasts are tall prismatic cells with well-developed RER and Golgi areas.
Figure 42. – Freeze-fracture. Gap junction between two hyposquamal scleroblasts.
Figure 43. – TEM. The innermost collagen fibrils and the Mts (arrow) located beneath the plasma membrane are shown in cross section.
Figure 44. – TEM. In this scleroblast, the outer side of the plasma membrane is connected with the collagen fibrils by a thin flocculent material and its inner side with a microfibrillar material (arrows).
Figures 45-46. – *Carassius auratus*. Indirect immunofluorescence visualising microtubules in the hyposquama.
Figure 45. – Control scales. **A**: Phase contrast. The double lines indicate the orientation of the innermost collagen fibrils. **B**: Tyr-tubulin Mts distribution. Note the similar orientation of tyrosinated Mts and the collagen fibrils in contact with the hyposquamal scleroblasts. mtoc: microtubule organizer centre.**C**: Glu-tubulin MTs distribution. Long curly microtubules arise from the MTOCs. Glu-tubulin labelled Mts are less numerous than the tyr-tubulin-labelled Mts.
Figure 46. – Four-day-regenerating scale. **A**: Phase contrast. The line indicates the orientation of the innermost collagen fibrils. **B**: Tyr-tubulin Mts distribution. Note the coalignment of the tyrosinated Mts with the innermost collagen fibrils. **C**: Glu-tubulin Mts distribution. Only the MTOCs are labelled

2012) or indentation and puncture testing were performed on individual scales (Zhu *et al*., 2012) or multiple scale layers (Zhu *et al*., 2013). The natural elasmoid scale assembly has inspired the fabrication of flexible protective composite systems (Vernerey and Barthelat, 2010; Browning *et al*., 2013; Chintapalli *et al*., 2014; Chua *et al*., 2016).

The protective high performance of the elasmoid scales is related to the hardness and stiffness of the superficial osseous layer and the softness and strength of the inner basal plate and a weak interface that allows delamination and the basal plate to stretch (Zhu *et al*., 2012; Dastjerdi and Barthelat, 2014). Studies focused on the puncture resistance of individual scales showed that elasmoid scales are superior to several engineered materials such as polystyrene and polycarbonate (Zhu *et al*., 2012).

Structures inspired by the scaled skin of teleosts could perhaps motivate the development of hybrid-mineralized materials that could trigger many engineering applications.

ELASMOID SCALES AS MODEL FOR BIOMEDICAL RESEARCH

Research trends in development of artificial tissues such as bone or corneas move towards the use of reliable animal models such as elasmoid scales. As for bone, fibrillar type I collagen is the main component of the matrix in the elasmoid scales and the hydroxyapatite crystals are coaligned with the collagen fibrils in the basal plate (Zylberberg and Nicolas, 1982). The organization of the collagen fibrils in a highly ordered three-dimensional lattice, akin to that of the cornea, makes them transparent. Their easily observed development facilitate study of real-time cellular activities on both faces of the scale.

Teleost elasmoid scales were considered to be useful in bone research (Yoshikubo *et al*., 2005; Brittijn *et al*., 2009; De Vrieze *et al*., 2010, 2011), since they are easy to collect in high numbers, and the removed scales regenerate trough processes consistent with data reported on bone osteogenesis (Bereiter-Hahn and Zylberberg, 1991). Scales were used to provide cells attached to their natural matrix for the study of bone physiology (Metz *et al*., 2012).

Because of their transparency and tensile strength, elasmoid scales treated for cell removal and demineralization to prevent immunogenicity were used as artificial cornea to seal corneal perforation (van Essenet *et al*., 2013; Yuan *et al*., 2014; Chen *et al*., 2015). Acellularised and decalcified scales were used as a scaffold for corneal regenerative applications. The circular groves of the outer surface form guiding channels for the cornea growing on the scaffold (Lin *et al*., 2010).

CONCLUDING COMMENTS

Structural investigations are required for a fundamental understanding of the relationship between the structure and the function of biomaterials that can inspire new bioengineering developments.

Acknowledgements. – I am greatly indebted to Dr. Michel Laurin for his constructive stylistic improvements and to Dr. François J. Meunier for providing micrographs.

REFERENCES

AGASSIZ L., 1833-1844. - Recherches sur les Poissons fossiles. Neuchatel: Petitpierre & Prince.

BAUDELOT M.M., 1873. - Recherches sur la structure et le développement des écailles des poissons osseux. *Arch. Zool. Exp. Gen.*, 2: 87-244; 429-480.

BELON DU MANS P., 1551. - Histoire naturelle des estranges Poissons marins… 119 p. Paris: Regnaud Chaudière.

BELON DU MANS P., 1555. - La Nature et la Diversité des Poissons, avec leurs Pourtraicts… 448 p. Paris: Charles Estienne.

BEREITER-HAHN J. & ZYLBERBERG L., 1991. - Regeneration of teleost fish scale. *Comp. Biochem Physiol.*, 105A: 625-641.

BERTIN L., 1944. - Modifications proposées dans la nomenclature des écailles et des nageoires. *Bull. Soc. Zool. Fr.*, 69: 198-202.

BRITTIJN S., DUIVESTEIJN S.J., BELMAMOUNE M. *et al.* [27 authors], 2009. - Zebrafish development and regeneration: new tools for biomedical research. *Int. J. Dev. Biol.*, 53: 835-850.

BROWN G.A. & WELLINGS S.R., 1969. - Collagen formation and calcification in teleost scales. *Z. Zellforsh.*, 93: 571-581.

BROWNING A., ORTIZ C. & BOYCE M.C., 2013. - Mechanics of composite elasmoid fish scale assemblies and their bioinspired analogues. *J. Mech. Behav. Biomed. Mat.*, 19: 75-86.

BURDAK V., 1979. - Morphologie fonctionnelle du tégument écailleux des Poissons. Kiev, La Pensée Scientifique, ed. [in Russian]. French translation. *Cybium*, 1986, 10(3) suppl.: 1-47.

BYERS H.R., FUJIWARA K. & PORTER K.R., 1980. -Visualization of microtubules of cells in situ by indirect immunofluorescence. *Proc. Natl. Acad. USA*, 77: 6657-6662.

CHEN S.C., TELINIUS N., LIN H.T., HUANG M.C., LINC. C., CHOU C.H. & HJORTDAL J., 2015. - Use of fish scale-derived biocornea to seal full-thickness corneal perforations in pig models. *PLOS ONE*, 10(11): e143511.

CHINTAPALLI R., MIRKHALAF M., DASTJERDI A.K. & BARTHELAT F., 2014. - Fabrication, testing and modeling of a new flexible armor inspired from natural fish scales and osteoderms. *Nat. Mat.*, 7: 748-756.

CHUA Y.S., LAW E., PANG S.D. & QUEK S.T., 2016. - Fish scale-cellular composite system for protection against low-velocity impact. *Comp. Struct.*, 145: 217-225.

COCKERELL T.D.A., 1911. - Note on the scales of the osteoglossid fishes. *Proc. Biol. Soc.* Washington, 24: 39.

CURREY J.D., 1999. - The design of mineralized hard tissues for their mechanicals functions. *J. Exp. Biol.*, 202: 3285-3294.

DANE P.J. & TUCKER J.B., 1986. - Supracellular microtubule alignments in cell layers associated with the secretion of certain fish scales. *J. Cell Sci.*, Suppl. 5: 273-291.

DASTJERDI A.K. & BARTHELAT F., 2014. - Teleost fish scales among the toughest collagenous material. *J. Mech. Behav. Biomed. Mat.*, 52: 95-107.

DELAMATER E.D. & COURTENAY W.R., 1974. - Fish scales as seen by scanning electron microscopy. *Fla. Sci.*, 37: 141-149.

DE VRIEZE E., METZJ.R. VON DEN HOFF J.W. & FLIK G., 2010. - TRAcP and cathepsin K in elasmoid scales: a role in mineral metabolism? *J. Appl. Ichthyol.*, 26: 210-213.

DE VRIEZE E., SHARIF F., METZ J.R., FLIK G. & RICHARDSON M.K., 2011. - Matrix metalloproteinases in osteoclasts of ontogenic and regenerating zebrafish scales. *Bone*, 48: 704-712.

FRANCILLON H. & MEUNIER F.J., 1985. - Conservation et présentation des préparations colorées au bleu alcian et à l'alizarine. *Cybium*, 9: 121-126.

FRIETSCHE R.A. & BAILEY C.F., 1980. - The histology and calcification of regenerating scales in the blackspotted topminnow, *Fundulus olivaceus* (Storer). *J. Fish Biol.*, 16: 693-700.

FROESE R. & PAULY D. (eds), 2017. - Fish Base. World Wide Web electronic publication. www.fishbase.org. Accessed Oct. 2017.

FROST H.M., 1969. - Tetracycline-based histological analysis of bone remodeling. *Calcif. Tiss. Res.,* 3: 211-237.

FROST H.M. & VILLANEUVA A.R., 1960. - Tetracycline staining of newly forming bone and mineralizing cartilage *in vivo*. *Stain Technol.*, 35: 135-138.

GABE M., 1968. - Techniques histologiques. 1113 p. Paris: Masson.

GARRANO A.M.C., LA ROSA G., ZHANG D., L.N. NIU, TAY F.R., MAJD H. & AROLA D., 2012. - On the mechanical behavior of scales of *Cyprinus carpio*. *J. Mech. Behav. Biomed. Mat.*, 7: 17-29.

GIRAUD M.M., CATANET J., MEUNIER F.J. & BOULIGAND Y., 1978. - The fibrous structure of coelacanth scales: a twisted 'plywood'. *Tissue Cell* 16: 217-236.

GOODRICH E.S., 1907. - On the scales of fish living and extinct, and their importance in classification. *Proc. Zool. Soc. Lond.*, 2: 751-774.

GUNDERSEN G.G., KALNOSKI M.H. & BULINSKI J.C., 1984 - Distinct populations of microtubules: Tyrosinated and nontyrosinated α-tubulins are distributed differently *in vivo*. *Cell*, 38: 779-789.

HUGHES D.R., 1981. - Development and organization of the posterior field of ctenoid scales in the Platycephalidae. *Copeia*, 3: 596-606.

IKOMA T., KOBAYASHI H., TANAKA J., WALSH D. & MANN S., 2003. - Microstructure, mechanical, and biomimetic properties of fish scales from *Pagrus major*. *J. Struct. Biol.,* 142: 327-333.

KHEMIRI S., MEUNIER F.J. LAURIN M. & ZYLBERBERG L., 2001. - Morphology and structure of the scales in the Gadiformes (Actinopterygii: Teleostei: Paracanthopterygii) and a comparison to elasmoid scales of other Teleotei. *Cah. Biol. Mar.*, 42: 345-362.

KLAATSCH H., 1890. - Zur Morphologie der Fischschuppen und zur Geschichte der Hartsubstanzgewebe. *Gegenbaurs Morphol. Jahrb.,* 16: 209-258.

KOBAYASHI H., 1952-1953. - Comparative studies of the scales in Japanese freshwater fishes, with special reference to phylogeny and evolution. *Jpn. J. Ichthyol.*, 2(4-5):183-191; 2(6): 246-260.

KOBAYASHI H., 1953-1954. - Comparative studies of the scales in Japanese freshwater fishes, with special reference to phylogeny and evolution. *Jpn. J. Ichthyol.*, 3: 83-86.

KOBAYASHI H., 1955. - Comparative studies of the scales in Japanese freshwater fishes, with special reference to phylogeny and evolution. *Jpn. J. Ichthyol.*, 4: 64-75.

LAGLER K.F., 1947. - Lepidological studies. I. Scale characters of the families of Great Lakes fishes. *Trans. Am. Microsc. Soc.*, 66: 149-171;

LANZING W.J.R. & HIGGINBOTHAM D.R., 1974. - Scanning microcopy of surface structures of *Tilapia mossambica* (Peters) scales. *J. Fish Biol.*, 6: 307-310.

LANZING W.J.R. & WRIGHT R.G., 1976. - The ultrastructure and calcification of the scales of *Tilapia mossambica* (Peters). *Cell Tissue Res.* 167: 37-47.

LE GUELLEC D. & ZYLBERBERG L., 1998. - Expression of type I and type V collagen mRNAs in the elasmoid scales of a teleost fish as revealed by *in situ* hybridization. *Connect. Tissue Res.*, 39: 257-267.

LILLIE R.D. & FULMER H.M., 1976 - Histopathologic Technic and Practical Histochemistry. 4th edit., 942 p. New York: McGraw-Hill Book Cie.

LIN C.C., RITCH R., LIN S.M., NI M.H., CHANG Y.C., LU Y.L., LAI H.J. & LIN F.H., 2010. - A new fish scale-derived scaffold for corneal regeneration. *J. Appl. Ichthyol.*, 19: 50-57.

LIPPITSCH E., 1990. - Scale morphology and squamation patterns in cichlids (Teleostei, Perciformes): a comparative study. *J. Fish Biol.*, 37: 265-291.

MAEKAWA K. & YAMADA J., 1970. - Some histochemical and fine structural aspects of growing scales of the rainbow trout. *Bull. Fac. Fish, Hokkaido Univ.*, 21: 70-78.

MAEKAWA K. & YAMADA J., 1972. - Morphological identification and characterization of cells involved in the growth of the goldfish scale. *Jpn. J. Ichthyol.*, 19: 1-10.

MANDL L., 1839. - Recherches sur la structure intime des écailles de poissons. *Ann. Sci. Nat. Zool.,* sér. II, 11: 337-371.

METZ J.R., DE VRIEZE E., LOCK E.J., SCHULTEN I.E. & FLIK G., 2012. - Elasmoid scales of fishes as model in biomedical bone research. *J. Appl. Ichthyol.*, 28: 382-387.

MEUNIER F.J., 1972. - Marquages simples et multiples du tissu osseux de quelques téléostéens par des substances fluorescentes. *C. R. Acad. Sci.*, 275: 1685-1688.

MEUNIER F.J., 1974. - La technique de marquage vital des tissus squelettiques des poissons. *Bull. Fr. Piscic.,* 255: 51-57.

MEUNIER F.J., 1984. - Spatial organization and mineralization of the basal plate of elasmoid scales in Osteichthyans. *Am. Zool.*, 24: 953-964.

MEUNIER F.J. & BOIVIN G., 1978. - Action de la fluorescéine, de l'alizarine, du bleu de calcéine et de diverses doses de tétracyclines sur la croissance de la truite et de la carpe. *Ann. Biol. Anim. Bioch. Biophys.*, 18: 1293-1308.

MEUNIERF.J. & CASTANET J., 1982. - Organization spatiale des fibres de collagène de la plaque basale des téléostéens. *Zool Scripta*, 11: 141-153.

MEUNIER F.J. & GÉRAUDIE J., 1980. - Les structures en contreplaqué du derme et des écailles des Vertébrés inférieurs. *Ann. Biol.*, 19: 1-18.

NEAVE F., 1936. - The development of scales of *Salmo*. *Trans. R. Soc. Can.*, 5: 55-72.

NEAVE F., 1940. - On the histology and regeneration of the teleost scale. *Quat. J. Microsc. Sci.*, 81: 541-568.

OHIRA Y., SHIMIZU M., URA K. & TAKAGI Y., 2007. - Scale regeneration and calcification in goldfish *Carassius auratus*: quantitative and morphological processes. *Fish Sci.*, 73: 46-54.

OMBREDANE D. & BAGLINIÈRE J.L., 1991. - Les écailles et leur utilisation en écologie halieutique. *In*: Tissus durs et Âge individuel des Vertébrés. Colloque National Bondy (Baglinière J.L., Castanet J., Conand F. & Meunier F.J., eds), pp. 151-192. Paris: ORSTOM and INRA.

ONOZATO H. & WATABE N., 1979. - Studies on fish scale formation and resorption. III. Fine structure and calcification of the fibrillary plate of the scales of *Carassius auratus* (Cypriniformes: Cyprinidae). *Cell Tissue Res*., 201: 409-422.

PAUTKE C., VOGT S., TISHER T., WEXEL G., DEPPE H., MILZ S., SCHIEKER M. & KOLK., 2005. - Polychrome labeling of bone with seven different fluorochromes: enhancing discrimination by spectral image analysis. *Bone*, 37: 441-445.

ROBERTS C.D., 1993. - Comparative morphology of spinned scales and their phylogenetic significance in the Teleostei. *Bull. Mar. Sci*., 52: 60-113.

RONDELET G., 1558. - L'Histoire entière des Poissons (1ère édition en Français, Mathieu Bonhomme, Lyon) 640 p. 2^{e} édit., 2002, CTHS Ed., Paris.

SCHÖNBÖRNER A.A., BOIVIN G. & BAUD C.A., 1979. - The mineralization processes in teleost fish scales. *Cell Tissue Res*., 202: 203-212.

SCHÖNBÖRNER A.A., MEUNIER F.J. & CASTANET J., 1981. - The fine structure of calcified Mandl's corpuscles in teleost fish scales. *Tissue Cell*, 13: 589-597.

SCHULTZE H.P., 1996. - The scales of Mesozoic actinopterygians. *In*: Mesozoic Fishes – Systematics and Paleoecology (Arratia G. & Viohl G., eds), pp. 83-93. Munich: Verlag Dr. Friedrich Pfeil.

SCHULTZE H.P., 2018. - Hard tissues in fish evolution: history and current issues. *Cybium*, 41(2): 29-39.

SIRE J.Y. & GÉRAUDIE J., 1983. - Fine structure of the developing scale in the Cichlid *Hemichromis bimaculatus* (Pisces, Teleostei, Perciformes). *Acta Zool*., 64: 1-8.

SIRE J.Y. & GÉRAUDIE J., 1984. - Fine structure of regenerating scales and their associated cells in the cichlid *Hemichromis bimaculatus* (Gill). *Cell Tissue Res*. 237: 537-547.

SIRE J.Y. & HUYSSEUNE A., 2003. - Formation of dermal skeletal and dermal tissues in fish: a comparative and evolutionary approach. *Biol. Rev*., 78:219-249.

SIRE J.Y., DONOGHUE P.C.J. & VICKARIOUS M.K., 2009. - Origin and evolution of the integumentary skeletonin non-tetrapod vertebrates. *J. Anat*., 214: 409-440.

SUDO S., TSUYUKI K., ITO Y. & IKOHAGI T., 2002. - A study on the surface shape of fish scales. *JSME Int. J. Ser. C-Mech. Syst. Mach. Elem. Manuf*., 45: 1100-1105.

VAN ESSENET T.H., LIN C.C., HUSSAIN A.K., MAAS S., LAI H.J., LINNARTZ H., VAN DEN BERG T.J., SALVATORI D.C., LUYTEN G.P. & JAGER M.J., 2013. - A fish scale derived collagen matrix as artificial cornea in rats: properties and potential. *Invest Ophthalmol. Vis Sci*., 54: 3224-3233.

VAN GAALEN S.M., KRUYT M.C., GEUZE R.E., DE BRUIJN J. D., ALBLAS J. & DHERT W.J.A., 2010. - Use of fluorochrome labels in *in vivo* bone tissue engineering research. *Tissue Eng*. Part B, 16: 209-217.

VAN OOSTEN J., 1957. - The skin and scales. *In*: The Physiology of Fishes. Vol. 1 (Brown M.E., ed.), pp. 207-244. New York, London: Academic Press.

VERNEREY F.J. & BARTHELAT F., 2010 - On the mechanics of fish scale structures. *Int. J. Solid. Struct*., 47: 2268-2275.

VORONINA E.P. & HUGHES D.R., 2013. - Types and development pathways of lateral line scales in some teleost species. *Acta Zool*., 94: 154-166.

WALLIN O., 1956. - Mucopolysaccharides and the calcification of the scale of the roach (*Leusciscus rutilus*). *Quart. J. Microsc. Sci*., 97: 329-332.

WATERMAN R.E., 1970. - Fine structure of scale development in the teleost, *Brachydanio rerio*. *Anat. Rec*., 168: 361-380.

WHITEAR M., 1986. - The skin of fishes including cyclostomes. Epidermis Dermis. *In*: Biology of the Integument: Vol. 2 (Bereiter-Hahn J., Matoltsy A.G. & Richards K.S., eds), pp. 8-64. Berlin, Heidelberg, New York, Tokyo: Springer Verlag.

WILLIAMSON W.C., 1851. - Investigations into the structure and development of the scales and bones of fishes. *Phil. Trans. R. Soc. Lond*., 141: 643-702.

YAMADA J., 1971. - A fine structural aspect of the development of scales in the chum salmon fry. Bull. *Jpn. Soc. Sci. Fish*., 37: 18-29.

YAMADA J. & WATABE N., 1979. - Studies on fish scale formation and resorption. I. Fine structure and calcification of the scales in *Fundulus heteroticlus* (Antheriniforles: Cyprinodontidae). *J. Morphol*., 159: 9-65.

YANG W., SHERMAN V.R., GLUDOVATZ B. *et al*. [11 authors], 2014. - Protective role of *Arapaima gigas* fish scales: Structure and mechanical behavior. *Acta Biomater*., 10: 3599-3614.

YOSHIKUBO H., SUZUKI N., TAKEMURA K., HOSO M., YASHIMA S., IWAMURO S., TAKAGI Y., TABATA M.J. & HATTORI A., 2005. - Osteoblastic activity and estrogenic response in the regenerating scale of goldfish, a good model of osteogenesis. *Life Sci*., 76: 2699-2709.

YUAN F., WANG L., LIN C.C., CHOU C.H. & LI L., 2014. - A corneal substitute derived from fish scale: 6 month follow up on rabbit model. *J. Ophtalmol*., 2014: 6 p. doi: 10.1155/2014/914542PMID: 25089206.

ZHU D., ORTEGA C.F., MOTAMEDI R., SZEWCIW L., VERNEREY F. & BARTHELAT F., 2012. - Structure and mechanical performance of a modern fish scale. *Adv. Eng. Mat*., 14: B185-B194.

ZHU D., SZEWCIW L., VERNEREY F. & BARTHELAT F., 2013. - Puncture resistance of the scaled skin from striped bass: collective mechanisms and inspiration for new flexible armor design. *J. Mech. Behav. Biomed. Mater*., 24: 30-40.

ZYLBERBERG L. & MEUNIER F.J., 1981. - Evidence of denticles and attachments fibres in the superficial layer of the scales of two fishes: *Carassius auratus* L., *Cyprinus carpio* L. (Cyprinidae, Teleostei). *J. Zool*., 195: 459-471.

ZYLBERBERG L. & MEUNIER F.J., 1996. - Ultrastructural data on the melanophores associated with the cellular elasmoid scales in *Leporinus friderici* (Teleostei: Ostariophysi: Anastomidae): their putative participation in scale matrix formation. *J. Morphol*., 228: 155-164.

ZYLBERBERG L. & NICOLAS G., 1982. - Ultrastructure of scales in a teleost (*Carassius auratus* L.) after use of rapid freeze-fixation and freeze-substitution. *Cell Tissue Res*., 223: 349-367.

ZYLBERBERG L., BEREITER-HAHN J. & SIRE J.Y., 1988. - Cytoskeletal organization and collagen orientation in fish scales. *Cell Tissue Res*., 253: 597-607.

ZYLBERBERG L., GERAUDIE J., MEUNIER F.J. & SIRE J.Y., 1991. - Biomineralization in the integumental skeleton of the living lower vertebrates. *In*: Bone, Vol. 4: Bone Metabolism and Mineralization (Hall B.K., ed.) pp. 171-224. Boca Raton: CRC Press.

ZYLBERBERG L., BONAVENTURE J., COHEN-SOLAL L. & BEREITER-HAHN J., 1992. - Organization and characterization of fibrillar collagens in fish scales *in situ* and *in vitro*. *J. Cell Sci*., 103: 273-285.